

# Heparin Promotes the Rapid Fibrillization of a Peptide with Low Intrinsic Amyloidogenicity

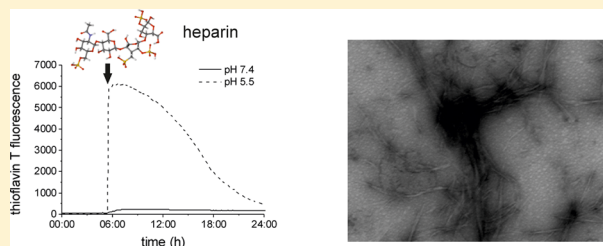
Jillian Madine,<sup>†</sup> Hannah A. Davies,<sup>†</sup> Eleri Hughes,<sup>‡</sup> and David A. Middleton<sup>\*,‡</sup>

<sup>†</sup>Institute of Integrative Biology, University of Liverpool, Crown Street, Liverpool L69 7ZB, United Kingdom

<sup>‡</sup>Department of Chemistry, Lancaster University, Lancaster LA1 4YB, United Kingdom

## S Supporting Information

**ABSTRACT:** Amyloid deposits *in vivo* are complex mixtures composed of protein fibrils and nonfibrillar components, including polysaccharides of the glycosaminoglycan (GAG) class. It has been widely documented that GAGs influence the initiation and progress of self-assembly by several disease-associated amyloidogenic proteins and peptides *in vitro*. Here we investigated whether the GAG heparin can serve as a cofactor to induce amyloid-like fibril formation in a peptide predicted to have a weak propensity to aggregate and not associated with amyloid disorders. We selected the 23-residue peptide PLB(1–23), which corresponds to the acetylated cytoplasmic domain of the phospholamban transmembrane protein. PLB(1–23) remains unfolded in aqueous solution for >24 h and does not bind thioflavin T over this time period, in agreement with computer predictions that the peptide has a very low intrinsic amyloidogenicity. In the presence of low-molecular mass (5 kDa) heparin, which binds PLB(1–23) with micromolar affinity, the peptide undergoes spontaneous and rapid assembly into amyloid-like fibrils, the effect being more pronounced at pH 5.5 than at pH 7.4. At the lower pH, peptide aggregation is accompanied by a transition to a  $\beta$ -sheet rich structure. These results are consistent with the polyanionic heparin serving as a scaffold to enhance aggregation by aligning the peptide molecules in the correct orientation and with the appropriate periodicity. PLB(1–23) is toxic to cells when added in isolation, and promotion of fibril formation by heparin can reduce the toxicity of this peptide, consistent with the notion that amyloid-like fibrils represent a benign end stage of fibrillization. This work provides insight into the role that heparin and other glycosaminoglycans may play in amyloid formation and provides therapeutic avenues targeting the reduction of cytotoxicity of species along the amyloid formation pathway.



Amyloid fibrils are classified by their characteristic cross- $\beta$  structure, in which  $\beta$ -strands are positioned perpendicular to the fibril axis and interchain hydrogen bonds are aligned approximately parallel to the fibril axis.<sup>1</sup> To date, 30 human proteins are associated with systemic or localized amyloid.<sup>2</sup> In addition, functional amyloids identified in a range of organisms, including insects, bacteria, fungi, and human skin, are thought to have evolved to exploit the strength and protease resistance properties of amyloid for biological purposes.<sup>3</sup> Moreover, some globular proteins when denatured can convert to fibrils, implying that an extended amyloidsome of proteins may be capable of assembling into amyloid-like fibrils under the appropriate conditions.<sup>4</sup> Several computational methods devised to predict the aggregation propensity of a given protein sequence provide a convenient starting point for exploring the size of the amyloids.<sup>5–7</sup>

Proteoglycans and glycosaminoglycans (GAGs) are extracellular matrix components that associate ubiquitously with amyloid deposits *in vivo*.<sup>8–10</sup> GAG mimetics are being evaluated clinically as Alzheimer's disease therapies<sup>11</sup> or for use as diagnostic agents.<sup>12</sup> Heparin is a highly sulfated GAG that has been shown to enhance the fibrillar assembly of several amyloidogenic proteins into fibrils, including  $\alpha$ -synuclein,<sup>13</sup> amylin,<sup>14</sup> transthyretin,<sup>10</sup> and tau,<sup>15</sup> by reducing the length of

the lag phase, enhancing elongation, and/or increasing fibril yield. It is becoming apparent that the acceleration of fibril formation can reduce the cytotoxicity associated with the intermediate species formed along the fibril formation pathway.<sup>16,17</sup> The enhancement of fibril formation may thus provide, in some cases, a therapeutic avenue for targeting amyloid-related diseases.<sup>18</sup> Heparin has also been shown to induce amyloid fibril formation by a range of hormone peptides,<sup>19</sup> suggesting that GAGs play a role in the storage of hormones as functional amyloid in secretory granules of the endocrine system. The helical protein apomyoglobin readily forms amyloid-like fibrils *in vitro* under conditions that destabilize the native fold, and Vilasi and co-workers<sup>20</sup> showed that heparin promotes fibrillization of folded wild-type apomyoglobin. It was suggested that the GAG–protein interaction is highly specific because alternating basic and nonbasic residues in the apomyoglobin turn regions are capable of binding heparin molecules.<sup>20</sup>

Here we investigated whether heparin could induce amyloid-like self-assembly *in vitro* by a normally unfolded peptide that

**Received:** September 5, 2013

**Revised:** November 25, 2013

**Published:** November 26, 2013

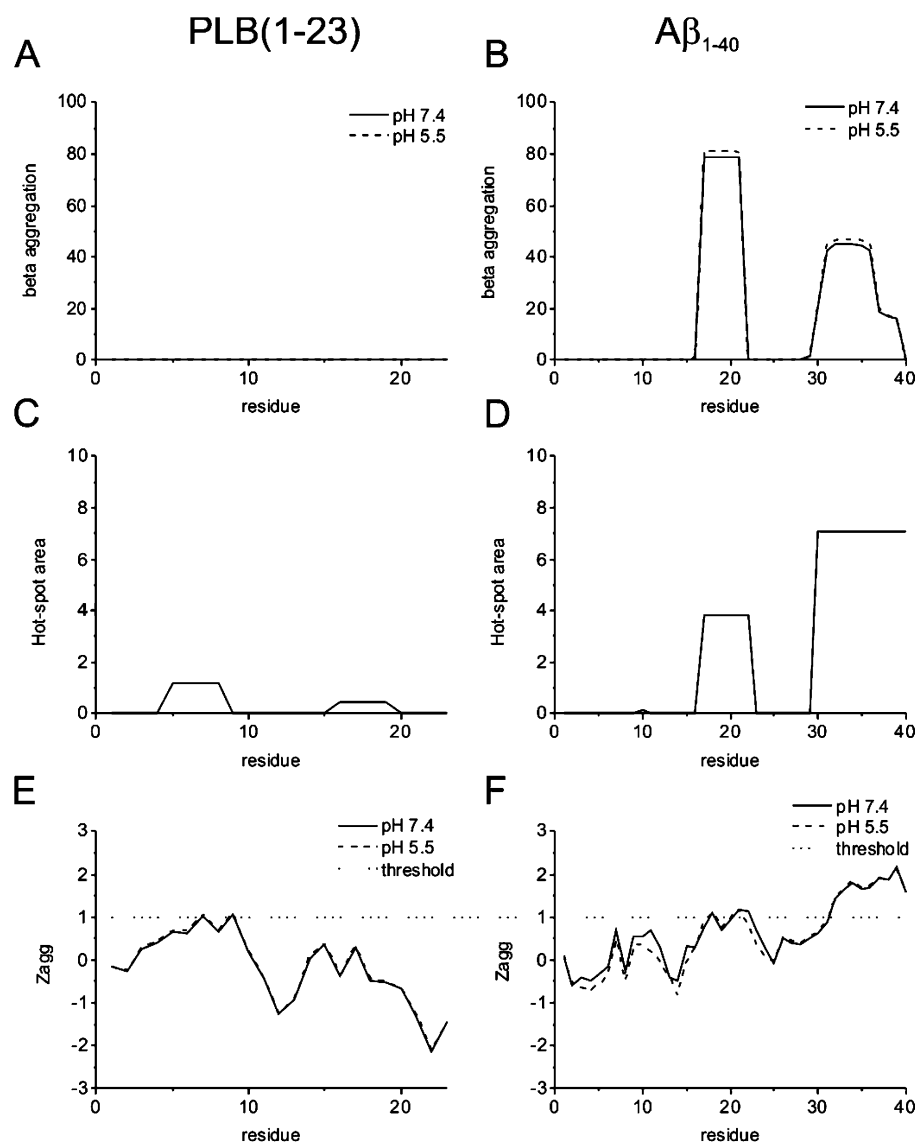


**Figure 1.** Amyloid propensity predictions for PLB(1–23) (left) and Aβ<sub>1–40</sub> (right) using TANGO (A and B), AGGRESCAN (C and D), and Zyggregator (E and F).

alone has a low intrinsic amyloidogenicity as determined by predictive and experimental methods. We chose the 23-residue peptide PLB(1–23), which corresponds to the natively N-terminally acetylated cytoplasmic domain of the phospholamban transmembrane protein that is expressed predominantly in the sarcoplasmic reticulum of cardiac myocytes.<sup>21</sup> PLB(1–23) has previously been shown to bind heparin-derived oligosaccharides with micromolar affinity.<sup>22</sup> The peptide is unstructured in aqueous solution and is predicted to have little or no propensity to spontaneously aggregate into amyloid-like fibrils, as we confirm experimentally here. We show that heparin induces virtually instantaneous fibrillization of PLB(1–23) and in doing so reduces the cytotoxicity associated with the soluble peptide. Although PLB(1–23) and heparin are not physiological binding partners, these results strengthen the argument that many, if not all, proteins can assemble into amyloid-like fibrils under suitable conditions, and with biological chaperones, and suggest that predictions of amyloidogenicity should consider GAG binding as a potential factor.

## METHODS

**Aggregation Prediction.** The sequences of PLB(1–23) and, for comparison, the amyloid-β peptide (Aβ<sub>1–40</sub>) were evaluated by three aggregation prediction servers. TANGO calculates a cross-β-aggregation propensity for each residue within the input sequence.<sup>7,23,24</sup> AGGRESCAN calculates an aggregation propensity value for each residue within the input sequence and provides a graphical output of the results.<sup>5</sup> Areas of the profile above a precalculated threshold are termed aggregation “hot spots”. Zyggregator calculates an aggregation profile of a sequence based on the physicochemical properties of its constituent amino acids.<sup>6,25</sup> Residues with a score of >1 are thought to promote aggregation of the sequence. TANGO and Zyggregator aggregation profiles were determined for the peptides at pH 7.4 and 5.5.

**Preparation of Peptide Solutions.** Ac-MEKVQYLTRS-AIRRASTIEMPQQ-NH<sub>2</sub> [PLB(1–23)] (95% pure) was purchased from Peptide Protein Research (Fareham, U.K.). The peptide was dissolved in 5% D-mannitol (pH 5.5)<sup>19</sup> or 20 mM sodium phosphate (pH 7.4 or 5.5) at a concentration of

2.0 mg/mL (0.72 mM). Additional samples were prepared using buffered solutions of low-molecular mass heparin [approximately 5 kDa (Fisher)] also at a concentration of 2.0 mg/mL (0.4 mM), or heparin disaccharide (Sigma) (0.4 mM). Samples were incubated at 37 °C while being shaken at 200 rpm for 5 days.

**Isothermal Titration Calorimetry.** Heat flow resulting from binding of low-molecular mass heparin to peptide was measured using a high-sensitivity VP-ITC MicroCalorimeter (MicroCal LLC, Northampton, MA). The reaction cell volume and total injection volume were 1.5 mL and 279.5  $\mu$ L, respectively. Experiments were performed at 25 °C, at a power reference setting of 15  $\mu$ cal/s (VP-ITC) with stirring at 307 rpm. Data analysis was conducted using Origin version 7 (MicroCal). The reaction cell contained a 50  $\mu$ M solution of peptide in 10 mM Tris and 1 mM EDTA (pH 7.4). A solution of heparin was prepared in the same buffer at a concentration of 250 or 500  $\mu$ M and injected via the syringe. Titrations were conducted at intervals of up to 10 min in 10  $\mu$ L aliquots following an initial discard aliquot of 3  $\mu$ L. Each injection generates a heat of reaction, determined by integration of the individual peaks from the heat flow trace. The heat of dilution was determined in control experiments whereby low-molecular mass heparin was titrated into a buffer solution without the peptide. Subtraction of the heat of dilution values from experimental values allows the determination of heat flow resulting from peptide binding.

**Thioflavin T Fluorescence.** Fluorescence was measured on a Flexstation 3 (Molecular Devices), with excitation at 430 nm and emission at 480 nm using clear bottom, black 96-well plates (Nunc) covered with a lid. Peptides were incubated at a concentration of 2 mg/mL with 20  $\mu$ M thioflavin T at 37 °C alone or with heparin at 2 mg/mL (0.4 mM) or heparin disaccharide at 0.4 mM. Readings were taken every 5 min while the samples were shaken for 5 s before each reading. Control wells of heparin with thioflavin T in each buffer were included on each plate. Experiments to examine the effect of salt on aggregation kinetics had 150 mM NaCl and 500 mM NaCl added to the buffers. An additional experiment was conducted in which heparin was added at 5.5 h to a final concentration of 2 mg/mL. Kinetics were analyzed assuming a sigmoidal growth curve, using the equation

$$F_t = F_0 + \frac{a}{1 + e^{-(t-T_i)/\tau}} \quad (1)$$

where  $F_t$  is the fluorescence at time  $t$ ,  $F_0$  is the initial fluorescence,  $F_m$  is the maximal fluorescence,  $T_i$  is the inflection point of the sigmoidal, and the slope  $1/\tau$  is the rate of polymerization.<sup>26</sup>

**Transmission Electron Microscopy.** Morphologies of the peptide solutions were analyzed by transmission electron microscopy (TEM) using negative staining with 4% uranyl acetate. Peptide suspensions (10  $\mu$ L) were loaded onto carbon-coated copper grids and visualized on a Tecnai 10 electron microscope at 120 kV.

**Circular Dichroism.** Samples were loaded into a quartz cuvette (Hellma), with a path length 0.2 mm, and the synchrotron radiation circular dichroism (SRCD) spectra were recorded from 190 to 260 nm on beamline B23, Diamond Light Source,<sup>27</sup> with 1 nm increments using a slit width of 0.5. Peptides were incubated at 2 mg/mL while being continuously shaken for up to 5 days at 37 °C and diluted to 0.5 mg/mL with buffer immediately prior to being transferred to the cuvette

(with shaking) to reduce sample absorbance. Spectra were recorded as the average of four scans and are presented following subtraction of buffer or heparin control spectra.

**Cell Viability.** SH-SY5Y cells (ATCC) were plated on 96-well plates at a density of 30000 cells/well and grown for 24 h. Peptide samples were diluted to 20  $\mu$ M in buffer and added to cells. Following incubation for 48 h, 10  $\mu$ L of the Cell Counting Kit-8 (CCK-8) solution was added and further incubated for 2 h, prior to measurement of the absorbance at 450 nm. The percentage cell viability was calculated from the absorbance of cells in the presence of the peptide with or without heparin measured relative to the absorbance of cells exposed to buffer alone or buffer containing 2 mg/mL heparin.

## RESULTS

PLB(1–23) is predicted to have a low intrinsic amyloidogenicity according to three predictive software packages: AGGRESCAN,<sup>5</sup> Zyggregator,<sup>6,25</sup> and TANGO.<sup>7,23,24</sup> All packages gave values below the thresholds for the predicted amyloidogenicity, which are shown in Figure 1 alongside predictions for  $A\beta_{1-40}$  for comparison. Zyggregator and TANGO aggregation profiles determined for the peptides at pH 7.4 and 5.5 showed no pH dependence (Figure 1A,E). TANGO allows the inclusion of the N-terminal acetyl and C-terminal amide groups, and these were predicted to have no appreciable effect on amyloidogenicity.

ITC was used to determine whether low-molecular mass heparin interacts with PLB(1–23) in aqueous solution (Figure 2). The ITC isotherm indicates that heparin binds to the

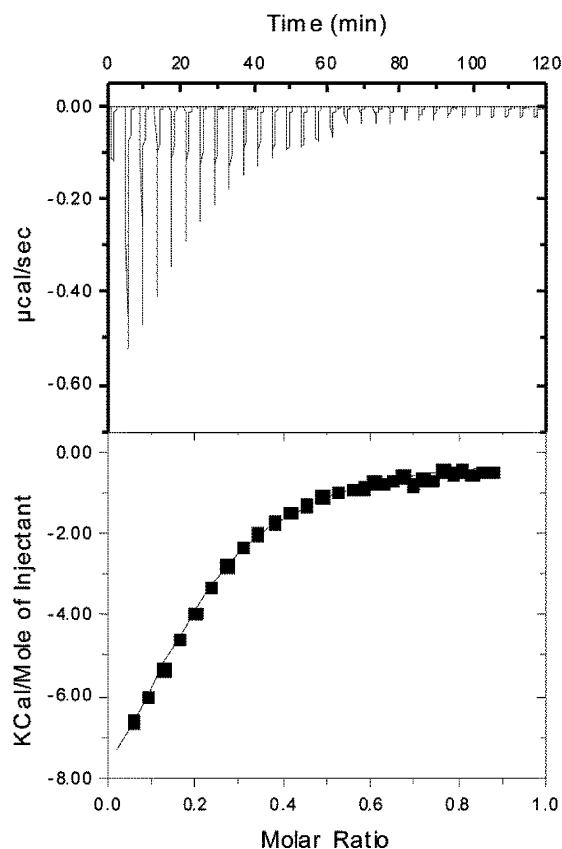


**Figure 2.** ITC data for 50  $\mu$ M PLB(1–23) titrated with heparin at 25 °C. Raw data of power vs time (top) and titration curves of integrated enthalpy vs reactant mole ratio (bottom).

peptide with an association constant ( $K_a$ ) of  $2.20 \times 10^5 \text{ M}^{-1}$ . Negative values for the change in binding enthalpy ( $\Delta H$ ) ( $-10.60 \text{ kcal/mol}$ ) and the change in entropy ( $\Delta S$ ) ( $-11.2 \text{ kcal K}^{-1} \text{ mol}^{-1}$ ) are consistent with electrostatic interactions and/or hydrogen bond formation. The stoichiometry ( $N$ ) of 0.18 indicates that each heparin molecule binds approximately five peptide molecules, presumably because of the large size and high charge of the saccharide ( $-18$  compared to  $+4$  for the peptide).

Several methods were used to investigate whether heparin increased the propensity of PLB(1–23) to aggregate. We initially employed the sample medium and concentrations reported by Maji and co-workers,<sup>19</sup> who showed that heparin induced amyloid-like fibril formation by a range of hormone peptides under these conditions. PLB(1–23) was dissolved to a concentration of  $2 \text{ mg/mL}$  ( $0.72 \text{ mM}$  peptide) in D-mannitol buffer (pH 5.5) alone or with  $2 \text{ mg/mL}$  ( $\sim 0.4 \text{ mM}$ ) low molecular-mass heparin. Samples were also prepared at the same concentrations in phosphate buffer (pH 7.4) for comparison. Thioflavin T fluorescence measurements were performed to monitor the aggregation properties of PLB(1–23) in the absence or presence of heparin. Incubation of PLB(1–23) alone at pH 5.5 or 7.4 did not enhance thioflavin T fluorescence over 24 h (Figure 3A, solid and dashed lines),

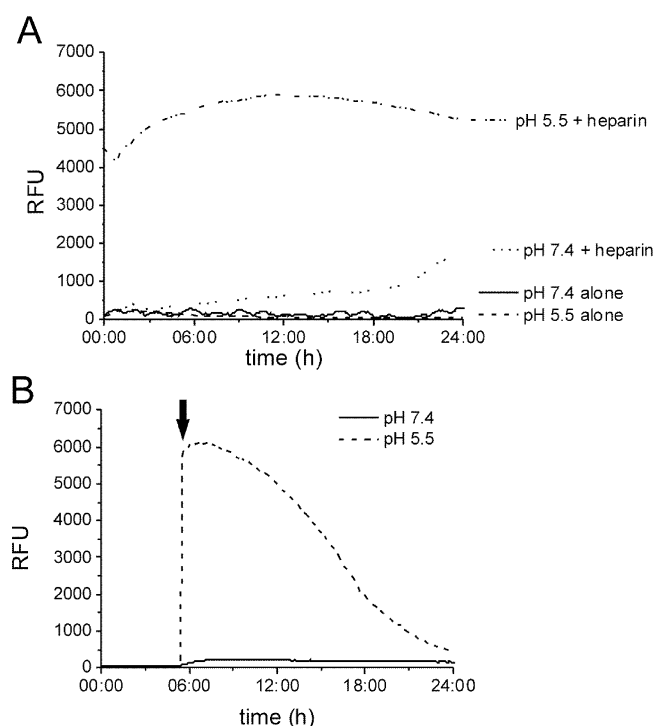


**Figure 3.** Time course of PLB(1–23) aggregation monitored by thioflavin T fluorescence. (A) Relative fluorescence units (RFU) at 480 nm for PLB(1–23) alone in phosphate at pH 7.4 (—), in D-mannitol at pH 5.5 (---), and in the presence of heparin in phosphate at pH 7.4 (···) and D-mannitol at pH 5.5 (---). (B) RFU upon addition of heparin added to PLB(1–23) after 5.5 h (black arrow) at pH 7.4 (—) and pH 5.5 (---). Data are averages of four repeats. Controls of heparin alone showed no increase in fluorescence over the time period examined.

suggesting that amyloid-like fibril formation did not occur over this time period. A small increase in ThT fluorescence [to  $\sim 1000$  relative fluorescence units (RFU)] in phosphate at pH

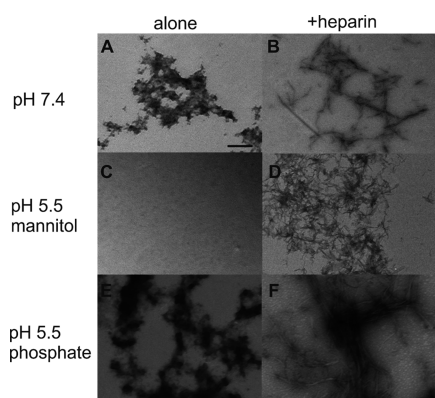
7.4 was observed after 30 h, but at pH 5.5, the fluorescence remained at the baseline until the measurement was stopped at 36 h (data not shown). Incubation of PLB(1–23) in the presence of heparin at pH 5.5 resulted in an enhanced thioflavin T fluorescence from the first measurement point onward (Figure 3A, dotted–dashed line). Incubation of PLB(1–23) in the presence of heparin at pH 7.4 resulted in a smaller increase in thioflavin T fluorescence, and after a lag period of approximately 20 h (Figure 3A, dotted line). We considered whether D-mannitol itself might play a role in inducing aggregation at pH 5.5, so a fresh sample was prepared in phosphate buffer at pH 5.5. In phosphate at pH 5.5, the thioflavin T fluorescence in the presence of heparin was enhanced from  $\sim 4000$  RFU from the initial measurement to  $>10000$  RFU after 24 h. In the absence of heparin, the relative fluorescence remained close to zero for 16.5 h, after which the fluorescence increased to  $\sim 4000$  RFU (Figure S1 of the Supporting Information). Hence, these data confirm that D-mannitol is not responsible for the rapid aggregation of PLB(1–23) in the presence of heparin, although in phosphate at pH 5.5 and 7.4 some aggregation occurs in the absence of heparin after incubation for several hours. All pH 5.5 samples presented henceforth were prepared in D-mannitol unless specified otherwise.

Figure 3A suggests that heparin at pH 5.5 rapidly catalyzes amyloid-like self-assembly<sup>28</sup> in the dead time of  $<1$  min that lapsed between mixing heparin with peptide and recording the first measurement. To test this supposition, the peptide was incubated with thioflavin T alone at pH 5.5 and heparin was automatically injected to a concentration of  $2 \text{ mg/mL}$  after 5.5 h (Figure 3B). The peptide remained stable for the first 5.5 h, with a baseline fluorescence in the absence of heparin. Immediately upon addition of heparin to the peptide, a rapid and striking increase (a rate of polymerization of  $113.3 \text{ h}^{-1}$ ) in fluorescence intensity was observed (Figure 3B, dashed line). The fluorescence enhancement at pH 5.5 was considerably greater than at pH 7.4, consistent with a higher level of conversion of the peptide to amyloid at the lower pH. The origin of the difference in behavior in the two pH conditions is not clear, as neither heparin nor the peptide contains groups (e.g., histidine) with  $pK_a$  values in this range.

The morphologies of the peptide solutions after incubation for 5 days were analyzed by TEM. In the absence of heparin, amorphous aggregates were formed in phosphate at pH 7.4 (Figure 4A), but nothing was visible on the grids following incubation in D-mannitol at pH 5.5 (Figure 4C). TEM analysis of the peptide solution incubated in the presence of heparin showed in both cases amyloid-like fibrils (Figure 4B,D). Fibrils at pH 5.5 were short and slender with dense coverage of the entire grid (Figure 4D). However, aggregates observed in phosphate at pH 7.4 were longer and needlelike, spanning lengths of up to  $1 \mu\text{m}$ , with a random distribution across the grid (Figure 4B). Incubation of PLB(1–23) for 5 days in phosphate at pH 5.5 resulted in amorphous aggregates in the absence of heparin (Figure 4E), but well-defined fibrils were observed in the presence of heparin (Figure 4F). Taken together, thioflavin T fluorescence and TEM indicate that although PLB(1–23) can under certain conditions precipitate as amorphous aggregates in the absence of heparin, amyloid-like fibril formation occurs only when the polysaccharide is present.

The low-molecular mass heparin used here has an average of 18 monosaccharide units, and it is tempting to envisage the repeating array of sulfate and acetate groups acting as a linear

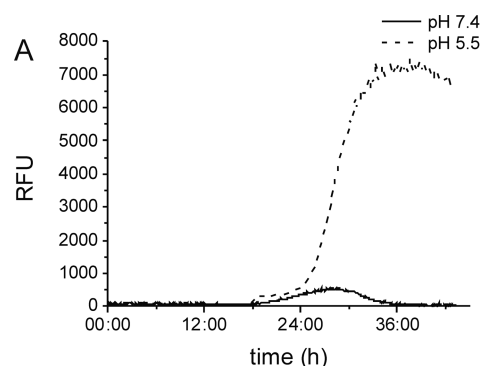




**Figure 4.** Transmission electron micrographs of PLB(1–23) (2 mg/mL) following incubation at 37 °C while being shaken for 5 days: (A) peptide alone in phosphate (pH 7.4), (B) peptide in phosphate (pH 7.4) in the presence of 2 mg/mL heparin, (C) peptide alone in D-mannitol (pH 5.5), (D) peptide alone in D-mannitol (pH 5.5) in the presence of 2 mg/mL heparin, (E) peptide alone in phosphate (pH 5.5), and (F) peptide in phosphate (pH 5.5) in the presence of 2 mg/mL heparin. The scale bar is 100 nm.

scaffold that initiates and propagates PLB(1–23) assembly through interactions with positively charged residues. If this were the case, lower degrees of heparin polymerization might thus be less effective at promoting peptide elongation. To test this hypothesis, PLB(1–23) was incubated with a heparin-derived disaccharide at the same molar concentration (0.4 mM), and hence the same peptide:saccharide charge ratio, used for low-molecular mass heparin. Intriguingly, the disaccharide did not induce immediate peptide aggregation as seen with low-molecular mass heparin, but an increase in ThT fluorescence did eventually occur after a lag phase of approximately 24 h, the enhancement in fluorescence being considerably higher at pH 5.5 than at pH 7.4 (Figure 5A). Under both pH conditions, PLB(1–23) assembles into a network of fibrous aggregates in the presence of the disaccharide, with the density of fibers being greater at pH 5.5 (Figure 5B). The negatively charged saccharide groups therefore appear to induce peptide aggregation regardless of the length of the saccharide chain, presumably as a result of charge neutralization resulting from ionic interactions between the saccharide sulfate and carboxyl groups and basic amino acid residues of the peptide. However, the longer saccharide chain of low-molecular mass heparin appears to immediately nucleate the rapid aggregation of the peptide, possibly because the number of repeating saccharide groups is optimal for templating peptide self-assembly.

To investigate the role of electrostatic interactions between the PLB(1–23) peptide and heparin, thioflavin T fluorescence was used to examine the effect of NaCl on the kinetics of PLB(1–23) aggregation. Intuitively, it would be expected that the salt would screen electrostatic interactions between heparin and the peptide and consequently prevent aggregation. A high (500 mM) concentration of NaCl induced a large increase in thioflavin T fluorescence (>8000 RFU) at pH 5.5 even in the absence of heparin, and the peptide precipitated as amorphous aggregates (Figure S2 of the Supporting Information). No evidence of aggregation was observed at pH 7.4 (data not shown). The high NaCl concentration alone appeared to be sufficient to cause protein aggregation and/or precipitation at pH 5.5, presumably through a typical “salting out” effect involving nonspecific Debye–Hückel screening or ionic



**B** pH 5.5 pH 7.4

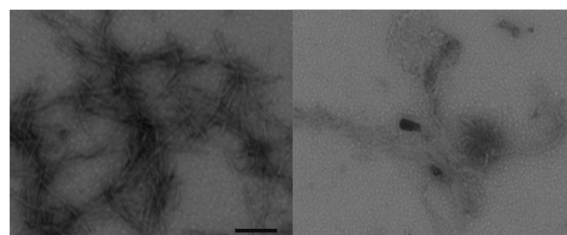


**Figure 5.** PLB(1–23) aggregation in the presence of 0.4 mM heparin disaccharide. (A) Thioflavin T fluorescence at 480 nm for PLB(1–23) at pH 7.4 (—) and pH 5.5 (---). (B) Transmission electron micrographs of the aggregates formed at pH 7.4 and 5.5. The scale bar is 100 nm.

interactions, for example. This effect of NaCl alone would make it difficult to interpret any effects of heparin in this medium, so further studies at this salt concentration are not reported here. At a lower, more physiologically relevant NaCl concentration of 150 mM, no increase in thioflavin T fluorescence occurred at pH 5.5 or 7.4 in the absence of heparin, indicating that the peptide is stable and does not aggregate under these conditions (Figure 6A, dotted–dashed or solid lines, respectively). Thioflavin T measurements in the presence of 0.4 mM heparin indicated that heparin promoted protein aggregation at pH 5.5 and 7.4, but the salt appeared to introduce a lag time of >3 h preceding an increase in fluorescence intensity (Figure 6A, dashed and dotted lines, respectively). This observation reflects the findings of Wang and co-workers, who reported that 150 mM NaCl lengthened by 3-fold the lag time for heparan sulfate-induced amyloid formation by a mutant of the islet amyloid polypeptide.<sup>29</sup> Here, TEM analysis of the NaCl solutions after 5 days in the presence and absence of heparin (Figure 6B) revealed morphologies similar to those of the aggregates formed in the absence of salt (Figure 4). Hence, it appears that electrostatic screening of PLB(1–23)–heparin interactions by NaCl impedes the formation of the critical nucleation state required for rapid elongation into fibrils but does not prevent fibril formation altogether.

We next investigated whether the process of aggregation was accompanied by changes in the peptide secondary structure. SRCD spectra were recorded for freshly prepared peptide samples and for samples after incubation with continuous agitation for 5 days. SRCD spectra of fresh solutions of the peptide in the absence of heparin at pH 5.5 and 7.4 (in the absence of salt) showed a minimal ellipticity at around 200 nm, consistent with a random coil (Figure 7A,B, solid lines). It is noted that the ellipticity values for fresh solutions prepared at

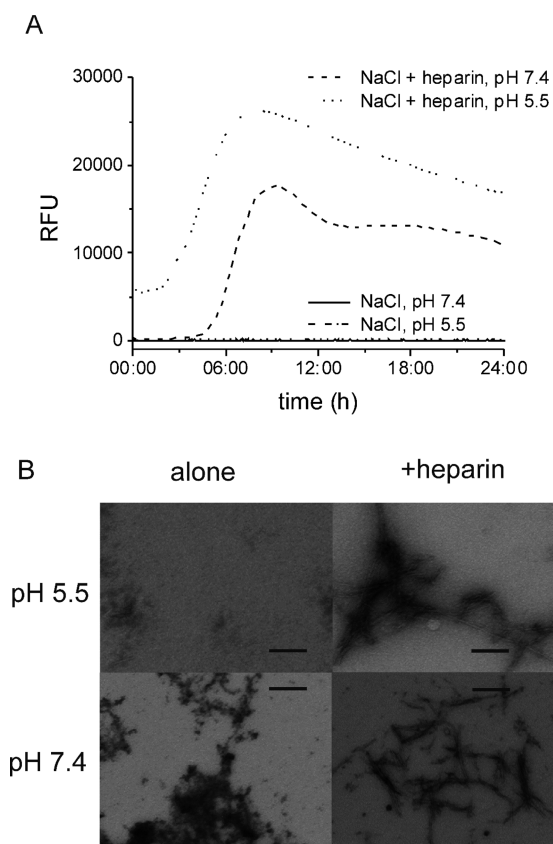


**Figure 6.** Effects of salt on the aggregation of PLB(1–23). (A) Thioflavin T analysis of 2 mg/mL PLB(1–23) alone or in the presence of 2 mg/mL heparin with 150 mM NaCl at pH 7.4 and 5.5. Data are averages of four repeats. Controls of heparin and salt alone showed no increase in fluorescence over the time period studied. (B) Transmission electron micrographs of the aggregates formed at pH 7.4 and 5.5 with 150 mM NaCl, in the absence and presence of heparin. The scale bar is 100 nm.

pH 7.4 and 5.5 are not the same, and this is attributed to slight differences in concentration and buffer signal strength. In the presence of heparin, spectra of fresh peptide solutions showed a slightly shifted minimal ellipticity of 2 nm at pH 7.4 and 5.5 (Figure 7A,B, dashed lines). The estimated secondary structure contents of the peptide in the presence and absence of heparin are summarized in Table 1. The SRCD spectrum of PLB(1–23) with heparin at pH 5.5 indicates a structural transition estimated to consist of 6%  $\beta$ -sheet and 26% turn that reflects the early enhancement of fluorescence observed in the thioflavin T measurements (Figure 3A). However, care should be taken in comparing these two independent measurements, particularly at the earliest stages of peptide aggregation. Although the dead time preceding the SRCD measurements on the freshly prepared samples was approximately the same as the dead time for the first thioflavin T readings, subtle differences in sample preparation conditions (e.g., the strength of agitation) could result in different nucleation times or rates of peptide self-assembly giving rise to the apparent discrepancy.

The SRCD spectra of PLB(1–23) alone after 5 days were consistent with the peptide remaining as a random coil at pH 7.4 and 5.5 (Figure 7A,B, dotted lines, and Table 1). After 5 days in the presence of heparin at pH 7.4, an overall loss of signal intensity was seen, which was attributed to a reduced concentration of the peptide in solution because of

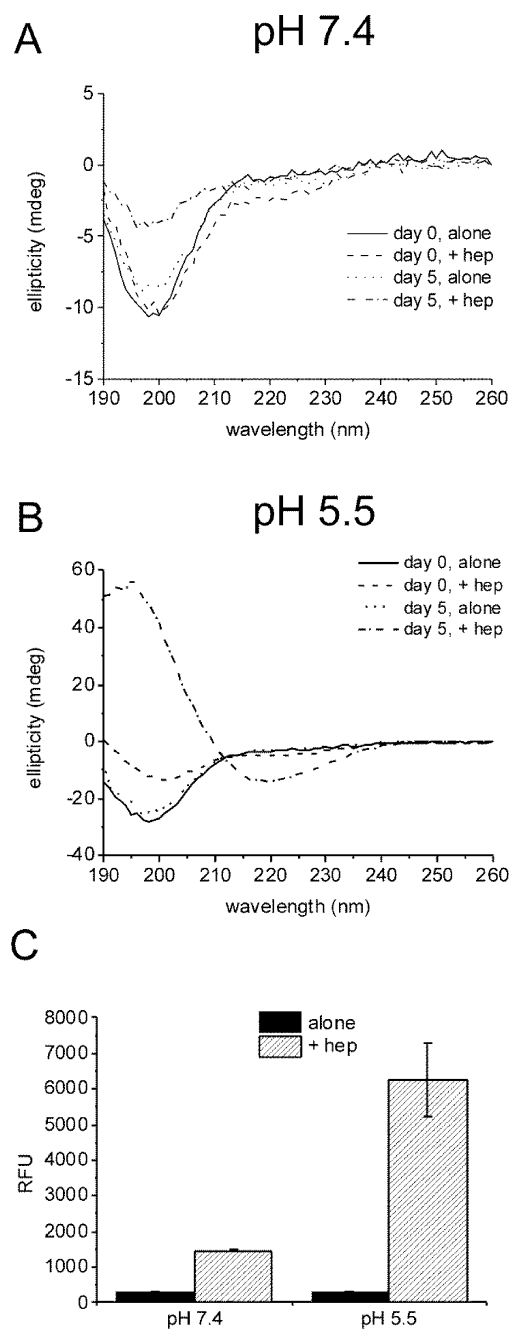


**Figure 7.** SRCD spectra of 2 mg/mL PLB(1–23) freshly prepared (day 0) and preincubated at 37 °C for 5 days, in the presence and absence of 2 mg/mL heparin. Spectra were recorded at pH 7.4 (A) and pH 5.5 (B) as an average of four scans following dilution to 0.5 mg/mL in buffer and are shown following subtraction of buffer and heparin control spectra. (C) Thioflavin T fluorescence of 2 mg/mL PLB(1–23) incubated for 5 days under the conditions used for SRCD analysis in the absence and presence of heparin at pH 7.4 or 5.5.

precipitation (Figure 7A, dotted–dashed line). With line fitting to the spectrum, it was estimated that approximately 54% of the peptide was  $\beta$ -sheet or turn on day 5 (Table 1). SRCD measurements for the peptide incubated in the presence of heparin at pH 5.5 for 5 days indicated that the peptide adopted virtually 100%  $\beta$ -sheet structure with a negative band between 210 and 220 nm and positive band between 195 and 200 nm (Figure 7B, dotted–dashed line, and Table 1), consistent with characteristic amyloid fibril structure.<sup>30</sup> Hence, the combination

**Table 1. Estimates of the Secondary Structure Content from SRCD Spectra of PLB(1-23) in Freshly Prepared Solutions (day 0) and after Incubation for 5 Days in the Presence and Absence of Heparin<sup>a</sup>**

conditions			secondary structure (%)			
time	pH	heparin	helix	sheet	turn	unordered
day 0	5.5	—	17	0	3	80
	5.5 <sup>b</sup>	+	19	6	26	48
	7.4	—	5	0	2	93
	7.4	+	5	1	0	94
day 5	5.5	—	25	3	3	68
	5.5	+	0	100	0	0
	7.4	—	4	1	5	90
	7.4	+	6	31	22	41

<sup>a</sup>Values were calculated by fitting the spectra using Olis Global Works secondary structure fitting software (CONTINLL algorithm) and basis sets 8, 10, and 11. The best fit was determined on the basis of the smallest normalized spectral fit standard deviation for the three basis sets (all values were  $\leq 0.07$  unless indicated). <sup>b</sup>Standard deviation of 0.11.

of a mildly acidic pH and the presence of heparin is sufficient for complete aggregation of PLB(1-23) into amyloid-like fibrils. Single-read thioflavin T analysis of these samples on day 5 showed virtually no enhancement of the fluorescence for the peptide in the absence of heparin but substantially higher fluorescence in the presence of heparin, the enhancement being greatest at pH 5.5 (Figure 7C). These measurements on day 5 reflect the differences in fluorescence observed at the 24 h end point of the time course measurements in Figure 3A and also the  $\beta$ -sheet/turn content of the peptide at day 5.

The cytotoxicity of PLB(1-23) to SHSY-5Y cells was tested using CCK-8 dye. Surprisingly, the soluble, wild-type peptide alone was toxic to cells, with observed cell death of approximately 60–70% upon addition of both freshly prepared peptide solutions and solutions preincubated for 5 days at pH 5.5 and 7.4 (Figure 8, black columns). It is not clear whether the cytotoxicity arises from soluble monomeric peptide or from

soluble oligomers that may formed under the conditions of the cell viability assay. However, peptide solutions with heparin present, both freshly prepared and preincubated under conditions comparable with those used for the experiments described above, showed a significant reduction in cytotoxicity regardless of pH or the duration of the preincubation of the peptide solution (Figure 8, shaded columns). This implies that heparin protects the cells from the toxic form(s) of PLB(1-23).

## DISCUSSION

The transition of soluble proteins and peptides to insoluble amyloid-like fibrils often involves destabilization of the native protein fold using extreme pH or temperature or the addition of a cofactor or denaturant.<sup>31–33</sup> However, not all proteins and peptides have an equally strong propensity to assemble from an unfolded state into amyloid fibrils. Here we have studied the effect of heparin as a cofactor to induce amyloid-like fibril formation in a natively unfolded peptide that is predicted to have low inherent amyloidogenicity. We show using ThT, SRCD, and TEM that PLB(1-23) remains stable in solution for >24 h, but low-molecular mass heparin induces rapid fibril formation of PLB(1-23), with the effect being most pronounced at pH 5.5. This peptide in its soluble form is toxic to SHSY-5Y cells when added in isolation, but heparin can reduce the cytotoxic effect. Previous findings with other peptides have indicated that amyloid-like fibrils represent a benign end stage of fibrillization that are not toxic to cells.<sup>16,34</sup> Whether heparin achieves its cytoprotective effect by enhancing the assembly of PLB(1-23) into inert amyloid-like fibrils or simply by masking the interactions of the peptide with the cells cannot be established at this stage.

PLB(1-23) is predicted to have low amyloidogenicity according to three independent computational methods, but incubation of the peptide alone in phosphate buffer for >16 h gives rise to enhanced thioflavin T fluorescence. The enhancement is substantially larger (and occurs after a shorter lag period) in the presence of 500 mM NaCl, which we attribute to the screening effect of the high salt concentration. In all these cases, however, the peptide is deposited as amorphous aggregates with no fibrillar structures in evidence. Remarkably, low-molecular mass (~5 kDa) heparin and the much smaller heparin-derived disaccharide, at concentrations of 0.4 mM, both induce formation of fibrillar PLB(1-23) aggregates. Peptide aggregation begins virtually instantaneously after the addition of 5 kDa heparin, whereas in the case of the disaccharide, fibril elongation is preceded by a lag phase that is typical of amyloidogenic proteins and peptides. Electrostatic effects undoubtedly play a role in PLB(1-23) aggregation, either at high salt concentrations or in the presence of heparin, but it would appear that the chemical structure of the polysaccharide, specifically the spatial distribution of anionic groups, is important for directing peptide self-assembly in a vectorial manner, culminating in the deposition of fibrous aggregates. Further studies with other naturally occurring or synthetic GAGs with different substitution patterns would help to test this hypothesis.

Heparin-derived oligosaccharides have previously been observed to interact with the PLB(1-23) peptide studied here.<sup>22</sup> Heparin binding regions usually contain consecutive basic residues described as BBXB or BBBXXB, where B is a basic residue and X is a hydrophobic residue.<sup>10,35</sup> It is therefore thought that heparin could associate with this peptide through

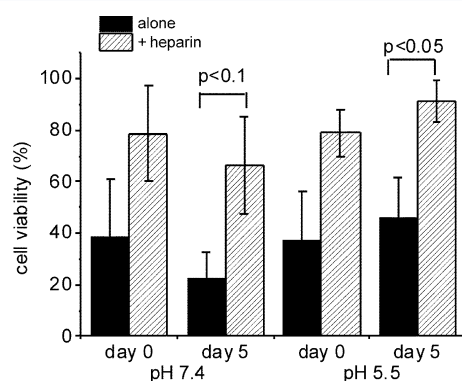


**Figure 8.** Cell viability of SHSY-5Y cells upon addition of PLB(1-23). The peptide was added to cells from a freshly prepared solution (day 0) and following preincubation for 5 days (day 5), at pH 7.4 and 5.5. The peptide was added to a final concentration of 20  $\mu$ M following preincubation at 2 mg/mL alone (black) and in the presence of 2 mg/mL heparin (shaded). Significant differences determined by a *t* test are shown. Data are means  $\pm$  the standard error for six independent wells. PLB(1-23) and heparin solutions preincubated for 5 days showed a significant reduction in cytotoxicity compared to peptide preincubated alone at pH 7.4 and 5.5 ( $p < 0.1$  and  $p < 0.05$ , respectively).



the arginine residues at positions 13 and 14. How the interaction invokes a disorder-to-order transition in the peptide is not clear, but one plausible explanation is that the repeating anionic groups of the saccharide units align the cationic peptide groups with a periodicity matching approximately the intermolecular hydrogen bond spacing of the cross- $\beta$  structure. Certainly, reducing the degree of saccharide polymerization from 18 to 2 units increases substantially the lag time preceding the onset of peptide self-assembly (Figure 5A). The very different effects on thioflavin T fluorescence intensity and SRCD observed secondary structure at two pH values suggested that heparin has a much more pro-amyloidogenic effect at pH 5.5 than at pH 7.4. Usually, a pH dependence is attributed to the protonation state of histidine residues providing an additional charged residue to enhance heparin binding,<sup>36,37</sup> as observed for transthyretin<sup>10</sup> and amyloid- $\beta$  peptides,<sup>36</sup> but this cannot explain our observations because the peptide lacks histidine. A decrease in pH has been shown to promote fibril formation in several amyloidogenic proteins, favoring the transition from nonfibrillar to fibrillar species. Destabilization of the native fold can occur at a reduced pH, resulting in partial denaturation and unfolding forming a species that readily assembles into amyloid fibrils as observed for transthyretin<sup>38</sup> and  $\beta_2$ -microglobulin<sup>39</sup> and due to the exposure of surface hydrophobic residues in prion proteins.<sup>40</sup> A model for fibrillogenesis of these proteins involving the association of partially unfolded molecules into ordered fibrillar assemblies has been proposed. A pH dependence of fibril formation has also been linked to the location of amyloid deposits within the body and the possible involvement of specific locations, e.g., lysosomes in amyloid-light chain disorder.<sup>41,42</sup> The wider biological implications of the results reported here are not yet known, so it is possible only to speculate at this stage. Interestingly, mutants of the glycoside hydrolase lysozyme, which catalyzes the hydrolysis of linkages between bacterial cell wall peptidoglycans, are associated with a familial form of amyloidosis.<sup>43</sup> Extrapolating the results of the work here, one could envisage that lysozyme aggregation might be promoted by interactions with the released bacterial glycan fragments. Investigations into lysozyme–GAG interactions may thus provide new insights into the aggregation of this well-characterized enzyme.

There is much interest in investigating the interactions between GAGs and amyloid fibers.<sup>14,44</sup> Here, we have shown that heparin can induce amyloid-like formation in a natively nonamyloidogenic peptide and that this effect is greater at pH 5.5 than at pH 7.4. Work on islet amyloid polypeptide aggregation has shown that the presence of GAGs may reduce the effectiveness of inhibitory compounds.<sup>29</sup> The data presented here provide an insight into the role that heparin and other GAGs may play in enhancing amyloid formation in a range of amyloid-related diseases and provide therapeutic avenues targeting the reduction of cytotoxicity of species along the amyloid formation pathway.

## ■ ASSOCIATED CONTENT

### ● Supporting Information

Additional figures showing the aggregation properties of PLB(1–23) under alternative buffer conditions. This material is available free of charge via the Internet at <http://pubs.acs.org>.

## ■ AUTHOR INFORMATION

### Corresponding Author

\*E-mail: [middletd@lancaster.ac.uk](mailto:middletd@lancaster.ac.uk). Telephone: +44 1524 594328.

### Funding

This work was funded by the Wellcome Trust (Grant 088563/B/09/Z).

### Notes

The authors declare no competing financial interest.

## ■ ACKNOWLEDGMENTS

We thank Diamond Light Source for access to beamline B23 (proposal SM8120) that contributed to the results presented here. We are grateful to Giuliano Siligardi and his team for their guidance.

## ■ REFERENCES

- (1) Sunde, M.; Serpell, L. C.; Bartlam, M.; Fraser, P. E.; Pepys, M. b., and Blake, C. C. F. (1997) Common core structure of amyloid fibrils by synchrotron X-ray diffraction. *J. Mol. Biol.* 273, 729–739.
- (2) Sipe, J. D., Benson, M. D., Buxbaum, J. N., Ikeda, S.-I., Merlini, G., Saraiva, M. J. M., and Westermark, P. (2012) Amyloid fibril protein nomenclature: 2012 recommendations from the Nomenclature Committee of the International Society of Amyloidosis. *Amyloid* 19, 167–170.
- (3) Fowler, D. M., Koulov, A. V., Balch, W. E., and Kelly, J. W. (2007) Functional amyloid: From bacteria to humans. *Trends Biochem. Sci.* 32, 217–224.
- (4) Goldschmidt, L., Teng, P. K., Riek, R., and Eisenberg, D. (2010) Identifying the amyloids, proteins capable of forming amyloid-like fibrils. *Proc. Natl. Acad. Sci. U.S.A.* 107, 3487–3492.
- (5) Conchillo-Sole, O., de Groot, N. S., Aviles, F. X., Vendrell, J., Daura, X., and Ventura, S. (2007) AGGRESCAN: A server for the prediction and evaluation of “hot spots” of aggregation in polypeptides. *BMC Bioinf.* 8, 65.
- (6) Tartaglia, G. G., and Vendruscolo, M. (2008) The Zyggregator method for predicting protein aggregation propensities. *Chem. Soc. Rev.* 37, 1395–1401.
- (7) Fernandez-Escamilla, A. M., Rousseau, F., Schymkowitz, J., and Serrano, L. (2004) Prediction of sequence-dependent and mutational effects on the aggregation of peptides and proteins. *Nat. Biotechnol.* 22, 1302–1306.
- (8) Ren, R., Hong, Z., Gong, H., Laporte, K., Skinner, M., Seldin, D. C., Costello, C. E., Connors, L. H., and Trinkaus-Randall, V. (2010) Role of Glycosaminoglycan Sulfation in the Formation of Immunoglobulin Light Chain Amyloid Oligomers and Fibrils. *J. Biol. Chem.* 285, 37672–37682.
- (9) Snow, A. D., Mar, H., Nochlin, D., Kimata, K., Kato, M., Suzuki, S., Hassell, J., and Wight, T. N. (1988) The presence of heparan sulfate proteoglycans in the neuritic plaques and congophilic angiopathy in Alzheimer's disease. *Am. J. Pathol.* 133, 456–463.
- (10) Noborn, F., O'Callaghan, P., Hermansson, E., Zhang, X., Ancsin, J. B., Damas, A. M., Dacklin, I., Presto, J., Johansson, J., Saraiva, M. J., Lundgren, E., Kisilevsky, R., Westermark, P., and Li, J.-P. (2011) Heparan sulfate/heparin promotes transthyretin fibrillization through selective binding to a basic motif in the protein. *Proc. Natl. Acad. Sci. U.S.A.* 108, 5584–5589.
- (11) Hawkes, C. A., Ng, V., and McLaurin, J. (2009) Small molecule inhibitors of A $\beta$ -aggregation and neurotoxicity. *Drug Dev. Res.* 70, 111–124.
- (12) Wall, J. S., Richey, T., Stuckey, A., Donnell, R., Macy, S., Martin, E. B., Williams, A., Higuchi, K., and Kennel, S. J. (2011) In vivo molecular imaging of peripheral amyloidosis using heparin-binding peptides. *Proc. Natl. Acad. Sci. U.S.A.* 108, E586–E594.



- (13) Cohlberg, J. A., Li, J., Uversky, V. N., and Fink, A. L. (2002) Heparin and other glycosaminoglycans stimulate the formation of amyloid fibrils from  $\alpha$ -synuclein *in vitro*. *Biochemistry* 41, 1502–1511.
- (14) Jha, S., Patil, S. M., Gibson, J., Nelson, C. E., Alder, N. N., and Alexandrescu, A. T. (2011) Mechanism of Amylin Fibrillization Enhancement by Heparin. *J. Biol. Chem.* 286, 22894–22904.
- (15) Goedert, M., Jakes, R., Spillantini, M. G., Hasegawa, M., Smith, M. J., and Crowther, R. A. (1996) Assembly of microtubule-associated protein tau into Alzheimer-like filaments induced by sulphated glycosaminoglycans. *Nature* 383, 550–553.
- (16) Arrasate, M., Mitra, S., Schweitzer, E. S., Segal, M. R., and Finkbeiner, S. (2004) Inclusion body formation reduces levels of mutant huntingtin and the risk of neuronal death. *Nature* 431, 805–810.
- (17) Madine, J., and Middleton, D. (2010) Comparison of aggregation enhancement and inhibition as strategies for reducing the cytotoxicity of the aortic amyloid polypeptide medin. *Eur. Biophys. J.* 39, 1281–1288.
- (18) Bodner, R. A., Outeiro, T. F., Altmann, S., Maxwell, M. M., Cho, S. H., Hyman, B. T., McLean, P. J., Young, A. B., Housman, D. E., and Kazantsev, A. G. (2006) Pharmacological promotion of inclusion formation: A therapeutic approach for Huntington's and Parkinson's diseases. *Proc. Natl. Acad. Sci. U.S.A.* 103, 4246–4251.
- (19) Maji, S. K., Perrin, M. H., Sawaya, M. R., Jessberger, S., Vadodaria, K., Rissman, R. A., Singru, P. S., Nilsson, K. P. R., Simon, R., Schubert, D., Eisenberg, D., Rivier, J., Sawchenko, P., Vale, W., and Riek, R. (2009) Functional Amyloids As Natural Storage of Peptide Hormones in Pituitary Secretory Granules. *Science* 325, 328–332.
- (20) Vilasi, S., Sarcina, R., Maritato, R., De Simone, A., Irace, G., and Sirangelo, I. (2011) Heparin Induces Harmless Fibril Formation in Amyloidogenic W7FW14F Apomyoglobin and Amyloid Aggregation in Wild-Type Protein *in Vitro*. *PLoS One* 6, e22076.
- (21) Fujii, J., Ueno, A., Kitano, K., Tanaka, S., Kadoma, M., and Tada, M. (1987) Complete complementary DNA-derived amino acid sequence of canine cardiac phospholamban. *J. Clin. Invest.* 79, 301–304.
- (22) Hughes, E., Edwards, R., and Middleton, D. A. (2010) Heparin-derived oligosaccharides interact with the phospholamban cytoplasmic domain and stimulate SERCA function. *Biochem. Biophys. Res. Commun.* 401, 370–375.
- (23) Linding, R., Schymkowitz, J., Rousseau, F., Diella, F., and Serrano, L. (2004) A comparative study of the relationship between protein structure and  $\beta$ -aggregation in globular and intrinsically disordered proteins. *J. Mol. Biol.* 342, 345–353.
- (24) Rousseau, F., Schymkowitz, J., and Serrano, L. (2006) Protein aggregation and amyloidosis: Confusion of the kinds? *Curr. Opin. Struct. Biol.* 16, 118–126.
- (25) Tartaglia, G. G., Pawar, A. P., Campioni, S., Dobson, C. M., Chiti, F., and Vendruscolo, M. (2008) Prediction of Aggregation-Prone Regions in Structured Proteins. *J. Mol. Biol.* 380, 425–436.
- (26) Alvarez-Martinez, M.-T., Fontes, P., Zomosa-Signoret, V., Arnaud, J.-D., Hingant, E., Pujo-Menjouet, L., and Liautard, J.-P. (2011) Dynamics of polymerization shed light on the mechanisms that lead to multiple amyloid structures of the prion protein. *Biochim. Biophys. Acta* 1814, 1305–1317.
- (27) Hussain, R., Javorfi, T., and Siligardi, G. (2012) Circular dichroism beamline B23 at the Diamond Light Source. *J. Synchrotron Radiat.* 19, 132–135.
- (28) Harper, J. D., and Lansbury, P. T. (1997) Models of amyloid seeding in Alzheimer's disease and scrapie: Mechanistic Truths and Physiological Consequences of the Time-Dependent Solubility of Amyloid Proteins. *Annu. Rev. Biochem.* 66, 385–407.
- (29) Wang, H., Cao, P., and Raleigh, D. P. (2013) Amyloid Formation in Heterogeneous Environments: Islet Amyloid Polypeptide Glycosaminoglycan Interactions. *J. Mol. Biol.* 425, 492–505.
- (30) Nelson, R., Sawaya, M. R., Balbirnie, M., Madsen, A. O., Christian, R., Grothe, R., and Eisenberg, D. (2005) Structure of the cross- $\beta$  spine of amyloid-like fibrils. *Nature* 435, 773–775.
- (31) Fändrich, M., Forge, V., Buder, K., Kittler, M., Dobson, C. M., and Diekmann, S. (2003) Myoglobin forms amyloid fibrils by association of unfolded polypeptide segments. *Proc. Natl. Acad. Sci. U.S.A.* 100, 15463–15468.
- (32) McParland, V. J., Kalverda, A. P., Homans, S. W., and Radford, S. E. (2002) Structural properties of an amyloid precursor of  $\beta_2$ -microglobulin. *Nat. Struct. Biol.* 9, 326–331.
- (33) Guijarro, J. I., Sunde, M., Jones, J. A., Campbell, I. D., and Dobson, C. M. (1998) Amyloid fibril formation by an SH3 domain. *Proc. Natl. Acad. Sci. U.S.A.* 95, 4224–4228.
- (34) Bodner, R. A., Housman, D. E., and Kazantsev, A. G. (2006) New directions for neurodegenerative disease therapy: Using chemical compounds to boost the formation of mutant protein inclusions. *Cell Cycle* 5, 1477–1480.
- (35) Cardin, A. D., and Weintraub, H. J. (1989) Molecular modeling of protein-glycosaminoglycan interactions. *Arteriosclerosis* 9, 21–32.
- (36) Brunden, K. R., Richter-Cook, N. J., Chaturvedi, N., and Frederickson, R. C. (1993) pH-dependent binding of synthetic  $\beta$ -amyloid peptides to glycosaminoglycans. *J. Neurochem.* 61, 2147–2154.
- (37) Elimova, E., Kisilevsky, R., and Ancsin, J. B. (2009) Heparan sulfate promotes the aggregation of HDL-associated serum amyloid A: Evidence for a proamyloidogenic histidine molecular switch. *FASEB J.* 23, 3436–3448.
- (38) Colon, W., and Kelly, J. W. (1992) Partial denaturation of transthyretin is sufficient for amyloid fibril formation *in vitro*. *Biochemistry* 31, 8654–8660.
- (39) McParland, V. J., Kad, N. M., Kalverda, A. P., Brown, A., Kirwin-Jones, P., Hunter, M. G., Sunde, M., and Radford, S. E. (2000) Partially unfolded states of  $\beta_2$ -microglobulin and amyloid formation *in vitro*. *Biochemistry* 39, 8735–8746.
- (40) Swietnicki, W., Petersen, R., Gambetti, P., and Surewicz, W. K. (1997) pH-dependent stability and conformation of the recombinant human prion protein PrP(90–231). *J. Biol. Chem.* 272, 27517–27520.
- (41) Rostagno, A., Vidal, R., Kaplan, B., Chuba, J., Kumar, A., Elliott, J. I., Frangione, B., Gallo, G., and Ghiso, J. (1999) pH-dependent fibrillogenesis of a V $\kappa$ III Bence Jones protein. *Br. J. Haematol.* 107, 835–843.
- (42) Khurana, R., Gillespie, J. R., Talapatra, A., Minert, L. J., Ionescu-Zanetti, C., Millett, I., and Fink, A. L. (2001) Partially folded intermediates as critical precursors of light chain amyloid fibrils and amorphous aggregates. *Biochemistry* 40, 3525–3535.
- (43) Pepys, M. B., Hawkins, P. N., Booth, D. R., Vigushin, D. M., Tennent, G. A., Soutar, A. K., Totty, N., Nguyen, O., Blake, C. C. F., Terry, C. J., Feast, T. G., Zalin, A. M., and Hsuan, J. J. (1993) Human lysozyme gene mutations cause hereditary systemic amyloidosis. *Nature* 362, 553–557.
- (44) Madine, J., Pandya, M. J., Hicks, M. R., Rodger, A., Yates, E. A., Radford, S. E., and Middleton, D. A. (2012) Site-Specific Identification of an A $\beta$  Fibril–Heparin Interaction Site by Using Solid-State NMR Spectroscopy. *Angew. Chem., Int. Ed.* 51, 13140–13143.